Colloid Polym Sci 279:727–735 (2001)

ORIGINAL CONTRIBUTION

K. Grundke
D. Pospiech
W. Kollig
F. Simon
A. Janke

Wetting of heterogeneous surfaces of block copolymers containing fluorinated segments

Received: 26 May 2000
Accepted: 3 January 2001

K. Grundke · D. Pospiech · W. Kollig
F. Simon · A. Janke
Institute of Polymer Research Dresden,
Hohe Strasse 6
01069 Dresden, Germany

K. Grundke (✉)
Institut für Polymerforschung
Dresden e.V., Hohe Strasse 6
01069 Dresden, Germany
e-mail: grundke@ipfdd.de
Tel.: +49-351-4658475
Fax: +49-351-4658-284

Abstract The wetting of well-characterized heterogeneous surfaces of block copolymers has been studied by low-rate dynamic contact angle measurements using axisymmetric drop-shape analysis. Atomic force microscopy (AFM) and X-ray photoelectron spectroscopy (XPS) were used to investigate the roughness, the heterogeneity and the chemical composition of the surfaces.
By changing the block length of polysulfone and semifluorinated polyester segments in the block copolymers, the surface heterogeneity of thin films prepared on silicon wafers could be controlled. Tapping-mode AFM measurements showed that soft, hydrophobic domains of varying size on the submicrometer length scale were obtained on these surfaces (60–250 nm). The mean roughness was of the order of several nanometers. The results of the contact angle measurements showed that neither roughness nor heterogeneity had a significant effect on the advancing contact angle of water, at the scale of the features present; however, the contact angle hysteresis increased with increasing percentage of the soft domains. We assume that liquid retention by the solid upon retraction of the three-phase line is the main cause for the observed increase in contact angle hysteresis. Concerning the molecular composition of these block copolymer surfaces, angle-resolved XPS analysis showed a surface segregation of fluorine within the surface region. A direct correlation was found between the fluorine content of the block copolymer surfaces and the advancing contact angle of water.

Key words Wetting · Axisymmetric drop shape analysis · Contact angle hysteresis · Heterogeneous surfaces · Block copolymers

Introduction

The wetting and adhesion properties of polymers with low-energy surfaces are important in numerous applications, such as protective coatings and materials with enhanced biocompatibility, and are a topic of appreciable scientific interest [1–12]. The synthesis of segmented block copolymers containing semifluorinated polyester segments offers a new strategy to obtain low-energy polymers with tailored surface properties. Owing to the ability of block copolymers to phase-separate, heterogeneous surfaces containing domains of different surface tension can be prepared systematically. Here, we use block copolymers consisting of semifluorinated polyester segments coupled to a polysulfone block.

Although it is well known that heterogeneous surfaces produce contact angle hysteresis, the causes for this phenomenon are not yet completely understood [13–17]. Contact angle hysteresis is not observed on certain well-prepared solid surfaces [18, 19]. The presence of domains of different surface tension, which vary in size, inhibits uniform wetting. It has been shown that contact angle hysteresis of heterogeneous surfaces is connected with contortions of the three-phase contact line caused by

hydrophobic or hydrophilic patches and that a positive line tension will tend to counteract the tendency towards these contortions [20]. On the basis of experimentally determined line tension values the lateral dimension of the patches for the generation of contact angle hysteresis could be in the micrometer range [21]. Recently, Fadeev and McCarthy [22] and Öner and McCarthy [23] studied the effects of topography length scales on wettability. From wettability studies on trialkylsilane monolayers covalently attached to silicon surfaces they concluded that molecular level topography (roughness and rigidity) contributes to contact angle hysteresis.

In this study, we used block copolymer surfaces prepared by spin-coating on silicon wafers to study experimentally the influence of the surface heterogeneity on the contact angle hysteresis of water. The roughness and heterogeneity of the surfaces were investigated by tapping-mode atomic force microscopy (AFM) with simultaneous topographical and phase detection [24–27]. In addition, the chemical composition of the block copolymer surfaces was studied by X-ray photoelectron spectroscopy (XPS) using angle-resolved XPS analysis. From the observed depth profiles of the surface F/C ratio and the comparison with the calculated bulk F/C ratio information on the fluorine surface segregation can be obtained.

Macroscopic advancing and receding contact angles of sessile liquid drops were measured using a contact angle technique based on axisymmetric drop shape analysis (ADSA) [28, 29]. In this way, contact angle hysteresis phenomena can be studied by measuring low-rate dynamic advancing and receding contact angles as a function of the location of the three-phase contact line. This technique eliminates the subjective error present in goniometer measurements and provides accurate values of the macroscopic contact angle from the profile coordinates of the drop [30–32].

It is the aim of this article to interpret experimentally observed macroscopic contact angle hysteresis on block copolymer surfaces in the context of the molecular structure and the chemical heterogeneity and roughness of these surfaces.

Experimental

Block copolymers

The chemical structures of the block copolymers under investigation are given in Scheme 1.

Formula 1: BCP 1 (p = 19.80) and BCP 2 (p = 4.67)

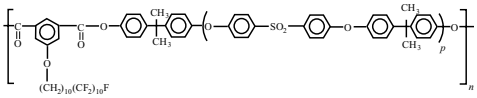

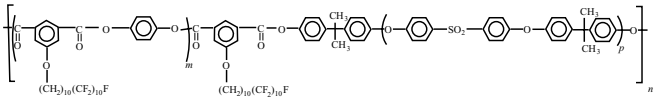

Formula 2: BCP 3 (p = 4.67)

Scheme 1 Chemical structure of the block copolymers investigated

The block copolymers BCP 1 and BCP 2 were synthesized by a transesterification polycondensation in the melt as described for other polysulfone block copolymers [33] using semifluorinated isophthalic acid and acetoxy-terminated polysulfone oligomers (see Appendix). The polymers obtained consist of polysulfone segments connected by semifluorinated isophthaloyl units and are, hence, non-phase-separated. For block copolymer BCP 3, semifluorinated isophthalic acid and 4,4′-phenylene diacetate were used in a 2:1 ratio, leading to a segment molecular weight of the semifluorinated polyester of 1750 g/mol. The formation of block copolymers was proven by ^{1}H and ^{13}C NMR spectroscopy as well as by gel permeation chromatography. The chemical characterization of the block copolymers is given in Table 1. BCP 3 shows phase separation into an amorphous polysulfone phase (glass transition detectable by differential scanning calorimetry and small-angle X-ray scattering) and an ordered phase of the semifluorinated polyester (melting and isotropization detectable).

Table 1 Chemical characterization of the segmented block copolymers under investigation

Block copolymer	Segment molecular weights			Molecular weights of the block copolymer[c]		
	M_n (g/mol) [a]	$M_{n,\ SF\text{-}PES}$ (g/mol)	Fluorine content (wt%)[b]	M_n (g/mol)	M_w (g/mol)	M_w/M_n
Semifluorinated polyester	–	–	42.72	22000[d]	–	–
Polysulfone	–	–	0	28000	48750	1.74
BCP 1	9000	840	4.06	20400	44000	2.16
BCP 2	2300	840	12.82	4500	10600	2.36
BCP 3	2300	3600[e]	19.98	16000	29000	1.82

[a] Determined by ^{1}H NMR and titration of OH end groups as described in Ref. [35]
[b] Calculated from the chemical composition (see formula)
[c] Determined by size-exclusion chromatography in cresol/chloroform using Waters Styragel HT3/HT6 columns; RI detection (for details see Ref. [12])
[d] Calculated from the ^{1}H NMR spectrum ($CDCl_3$)
[e] Calculated from the ratio of semifluorinated isophthalic acid and hydroquinone diacetate used in the polycondensation reaction

Preparation of thin films

The block copolymer films were prepared on top of oxide-covered Si (100) surfaces (Wacker Siltronic, Germany) by spin-coating (Headway, USA; 2000 rpm for 30 s) a 2 wt% solution of the block copolymer in a chloroform/pentafluorophenol mixture (50/50 v/v). The solutions were filtered using a 200-nm filter. After spin-coating, the block copolymer films were annealed for 4 h at 180 °C in a vacuum.

We used thermally oxidized wafers. The thickness of the oxide layer was 54 nm as determined by ellipsometry. Prior to spin-coating, the silicon substrates were cleaned by a wet chemical treatment in a freshly prepared hot (80 °C) piranha solution [H_2SO_4/30% H_2O_2 (4:1)] for 60 min, rinsed in deionized water and dried for 12 h at 30 °C in a vacuum.

Methods

Contact angle measurements using ADSA

The ADSA-profile (ADSA-P) was used to measure advancing and receding contact angles. The ADSA-P is a technique to determine liquid–fluid interfacial tensions and contact angles from the shape of axisymmetric menisci, i.e., from sessile as well as pendant drops. The strategy employed is to fit the shape of an experimental drop to the theoretical drop profile according to the Laplace equation of capillarity,

$$\Delta P = \gamma\left[\frac{1}{R_1}+\frac{1}{R_2}\right] \ , \qquad (1)$$

using the surface (interfacial) tension, γ, as one of the adjustable parameters; ΔP is the pressure difference across the liquid and fluid phases, and R_1 and R_2 are the two principal radii of curvature of the drop. The best fit identifies the correct interfacial tension and, in the case of a sessile drop, the contact angle. Details of the methodology can be found in Ref. [28].

Apart from local gravity and the densities of the liquid and fluid phases, the only information required by ADSA is several arbitrary but accurate coordinate points selected from the drop profile. An automatic digitization technique utilizing digital image acquisition and analysis was used. Computer software has been developed to implement this method and the computational results provide the values of the interfacial tension, the drop volume, the surface area, the contact angle and the radius of the three-phase contact line [29]. A Sun workstation was used to acquire images from the image processor and to perform the image analysis and computation.

Low-rate dynamic contact angle experiments were carried out by supplying liquid to the sessile drop from below the solid surface through a hole of about 1 mm diameter in the substrate using a motorized syringe device [30]. At first, the motorized syringe mechanism was set to a specific speed and the syringe plunger was pushed, leading to an increase in the drop volume and, hence, the three-phase contact radius. Then, liquid was withdrawn so that the drop volume was decreased. A sequence of pictures of the growing and shrinking drop was recorded by the computer typically at a rate of one picture every 2–5 s. For each low-rate dynamic contact angle experiment, 250–500 images were normally taken.

X-ray photoelectron spectroscopy

XPS measurements were carried out by means of an ESCAlab 220i spectrometer (Vacuum Generator, UK) equipped with a non-monochromatized Mg Kα X-ray source with a primary energy of $h\nu = 1253.6$ eV. All spectra were adjusted to the hydrocarbon reference peak C 1*s* at a binding energy of 285.00 eV. The take-off angle, θ, is defined here as the angle between the sample surface normal and the electron optical axis of the spectrometer. Take-off angles correspond to the information depth according to $\lambda_i = \lambda_i^0 \cos\theta$, where λ_i is the effective escape depth and λ_i^0 is the inelastic mean free path of the electrons for a given energy and material. The λ_i^0 value of carbon (C 1*s* peak) in organic polymers is about 12 Å, i.e., the information depth approaches $3\lambda_i^0$ [34].

Atomic force microscopy

AFM experiments were performed in tapping mode under ambient conditions using a Nanoscope IIIa BioScope from Digital Instruments, Santa Barbara. POINTPROBE silicon cantilevers for force modulation mode from Nanosensors, Germany, (resonance frequency 75 kHz, force constant 2.8 N/m) were used for both height and phase imaging. In accordance with Magonov et al. [27] the scan conditions were chosen to reveal stiffness contrast in the phase image (free amplitude, $A_0 > 100$ nm, setpoint ratio, $r_{sp} \sim 0.5$) and adhesion contrast-phase imaging ($A_0 < 20$ nm, $r_{sp} \sim 0.7$). Under these conditions, soft areas in the images appear dark and hard areas appear bright.

Height images for roughness measurements were recorded in soft tapping mode ($r_{sp} \sim 0.9$). A three-dimensional mean roughness parameter, S_a, was calculated using the following equation:

$$S_a = \frac{1}{L_x L_y}\int_0^{L_y}\int_0^{L_x} |f(x,y)|\mathrm{d}x\,\mathrm{d}y \ , \qquad (2)$$

where $f(x, y)$ is the surface relative to the center plane and L_x and L_y are the dimensions of the surface.

Variable angle spectroscopic ellipsometry

Variable angle spectroscopic ellipsometry was performed using a rotation analyzer type variable-angle multiwavelength instrument (Woolam M44 ellipsometer, Lincoln, Neb.) to determine the thickness of the block copolymer films. Typical thickness values of the block copolymer films determined by ellipsometry were in the range 80–160 nm.

Results

ADSA-P measurements

Two typical examples of low-rate dynamic contact angle experiments for the block copolymer BCP 3 (Table 1) are shown in Fig. 1. As can be seen in this figure, four parameters were measured simultaneously: the drop volume, V, the three-phase contact radius, R, the contact angle, θ, and the liquid surface tension, γ_{lv}, of the sessile drop. Increasing the V linearly by continuously pumping the liquid into the drop with the motorized syringe causes the three-phase contact line to advance with θ essentially constant as R increases. The approximate rate of advancing can be determined by linear regression from the linear region of the plot of the three-phase contact radius, R, over time. In the specific example given in Fig. 1a the drop periphery was advanced at a rate of 0.196 mm/min.

The constancy of the contact angles with increasing R indicates that θ is independent of the location of the

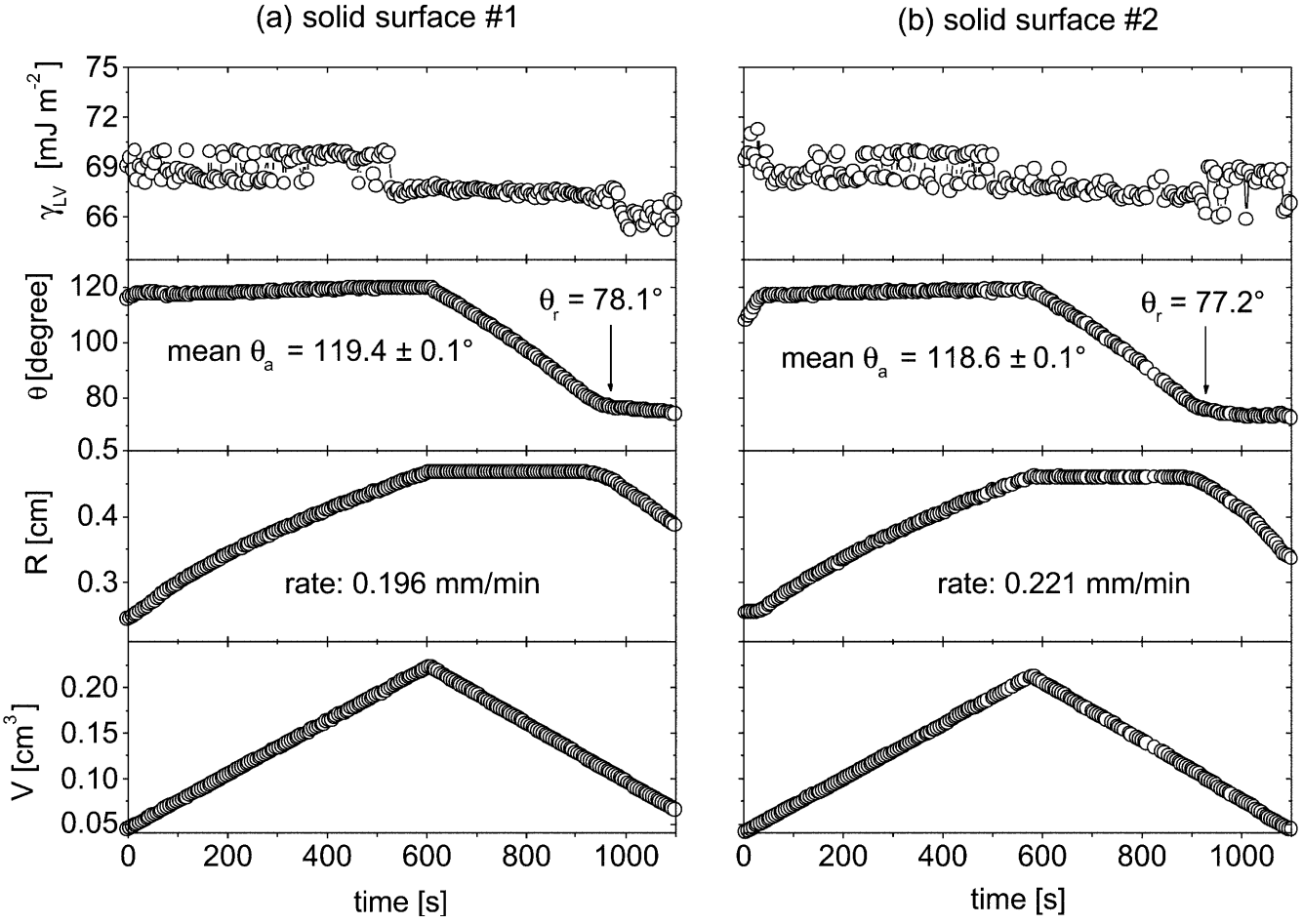

Fig. 1 Low-rate dynamic contact angles of water on block copolymer BCP 3 measured by axisymmetric drop shape analysis-profiles. γ_{lv}, θ, R, and V are, respectively, the liquid–vapor surface tension, the contact angle, the three-phase contact radius, and the drop volume

contact line on the block copolymer surface. The advancing contact angles were averaged, after R reached 0.4 cm to yield a mean advancing contact angle of 119.4 ± 0.1°. The error limit is the 95% confidence interval. The reproducibility of this solid–liquid system is shown in Fig. 1b for a different, newly prepared film using the same block copolymer as in Fig. 1a (BCP 3) at a slightly different rate of advancing of 0.221 mm/min. The mean advancing θ in this experiment is found to be 118.6 ± 0.1°. A summary of the advancing contact angles measured on all the block copolymers investigated is given in Table 2. For each block copolymer, two or three newly prepared films were used. It should be mentioned that the error limits (95% confidence interval) for the mean advancing contact angles for each individual run are very small, typically in the range 0.1–0.2°. This is in part due to the fact that very large numbers of individual contact angles, each for a new drop, can be acquired in a run. However, the errors from averaging over all runs are larger. Presumably, this is due to the fact that in spite of all the care taken with the preparation of the films, there is a somewhat larger variability from film to film than for an individual film.

The results (Table 2) show that the mean advancing contact angle calculated from the measurements on different films is distinctly higher for the block copolymer BCP 3. In the case of BCP 1 and BCP 2, the advancing contact angles yield lower values. Considering the standard deviations, the mean contact angles for these two block copolymers are not distinguishable.

Generally, the measured advancing contact angles on the block copolymer surfaces are between the values of the pure semifluorinated polyester homopolymer ($\theta_a = 125°$) and the pure high-molecular weight polysulfone ($\theta_a = 103.5°$) [35].

If the liquid is withdrawn steadily from the sessile drop, a linear decrease in the drop volume and the contact angle is caused, while the contact radius is constant (Fig. 1). At a certain point marked in Fig. 1 the three-phase contact line begins to recede and receding contact angles could be measured. In contrast to the advancing angles, the receding contact angles measured were not constant over time. To determine the contact angle hysteresis, the difference was calculated between

Table 2 Summary of water contact angles on three different multiblock copolymer surfaces. The roughness and heterogeneity of the surfaces were determined by atomic force microscopy

Block copolymer	Contact angles measured by ADSA-P			Roughness S_a (10×10 μm) (nm)	Heterogeneity Mean domain diameter (nm)	Surface ratio of soft domains (%)
	θ_a (deg)	θ_r (deg)	$\Delta\theta$ (deg)			
BCP 1	113.4 ± 0.04	89.4	24,0	0.9	66	3.5
	109.9 ± 0.1	83.5	26.4			
Mean	*111.6 ± 2.5*	*86.5 ± 4.2*	*25.1 ± 1.7*			
BCP 2	114.0 ± 0.2	84.8	29.2	11.3	242	5.5
	114.1 ± 0.2	82.0	32.1			
	111.9 ± 0.1	83.0	28.9			
Mean	*113.3 ± 1.2*	*83.2 ± 1.4*	*30.1 ± 1.8*			
BCP 3	118.2 ± 0.1	81.0	37.2	4.9	109	8.5
	118.6 ± 0.1	77.2	41.4			
	119.4 ± 0.1	78.1	41.3			
Mean	*118.7 ± 0.6*	*78.8 ± 2.0*	*39.9 ± 2.4*			

the mean advancing contact angle and the receding angle that was measured when the three-phase contact line began to retract. Since the time of contact of the liquid with the solid surface cannot be controlled exactly in our experiments the contact time of the liquid was different as is shown in Fig. 1. Owing to these experimental difficulties the receding angle must be considered as a semiquantitative parameter. The receding angles for the two different surfaces were determined to be 78.1° and 77.2°.

As can be seen from Table 2, the mean values of the receding angles on the different block copolymer surfaces show an opposite tendency compared to the advancing contact angles: higher receding angles were determined on block copolymers BCP 1and BCP 2. Thus, the contact angle hysteresis increases from block copolymer BCP 1 to BCP 3.

The fact that the advancing water contact angles are essentially indistinguishable for BCP 1 and BCP 2 is, at first sight, very surprising, since the relative amounts of the semifluorinated polyester segment and the polysulfone segment are different in the block copolymer bulks (Table 1). It was, therefore, investigated by XPS analysis whether or not the elemental composition near the surface is comparable to the elemental composition in the bulk.

Angle resolved XPS analysis

Angle dependent XPS was used to quantify the chemical surface composition of the different block copolymers. The information depth was varied by collecting data at take-off angles between the sample surface and the analyzer of 0°, 45° and 60°. These angles correspond to information depths of 3.5, 2.5 and 1.7 nm, respectively. A typical survey scan of block copolymer BCP 2 at a take-off angle of 60° is shown in Fig. 2.

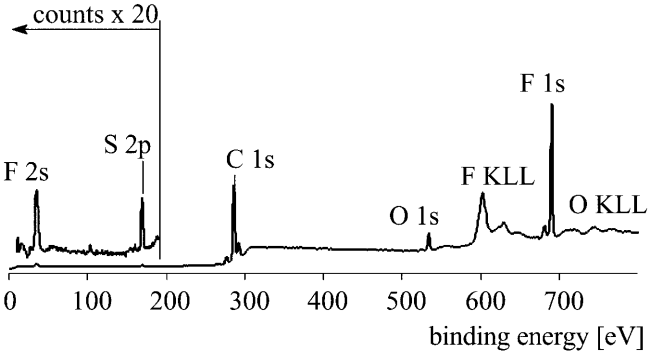

Fig. 2 X-ray photoelectron spectroscopy (*XPS*) survey spectrum of block coplymer BCP 2 taken at a take-off angle of 60°

From the peak areas shown in this spectrum, quantitative elemental compositions were determined. The F/C and S/C ratios versus the information depth are given in Fig. 3 for the three block copolymers investigated.

It can be seen that the F/C ratio is increased with decreasing sampling depth whereas the S/C ratio is decreased towards the outer surface. From these results it can be concluded that there is a fluorine surface segregation within the surface region. The calculated F/C bulk ratios are 0.16 for BCP 3, 0.12 for BCP 2 and 0.03 for BCP 1, respectively. The comparison of the F/C ratios obtained by XPS (Table 3) with these bulk F/C ratios gives additional indication of the relative F/C enrichment in the surface region of the block copolymers investigated.

Though the bulk fluorine content of block copolymers BCP 1 and BCP 2 is very different (Table 1) the XPS study shows that the elemental composition near the surface is essentially the same for both block copolymers (Fig. 3, Table 3), and the advancing contact angles register this fact. The distinctly higher advancing

contact angles on block copolymer BCP 3 correlate with the higher fluorine concentration in the surface region. Compared to the other block copolymers, BCP 3 also has the highest fluorine content in the bulk.

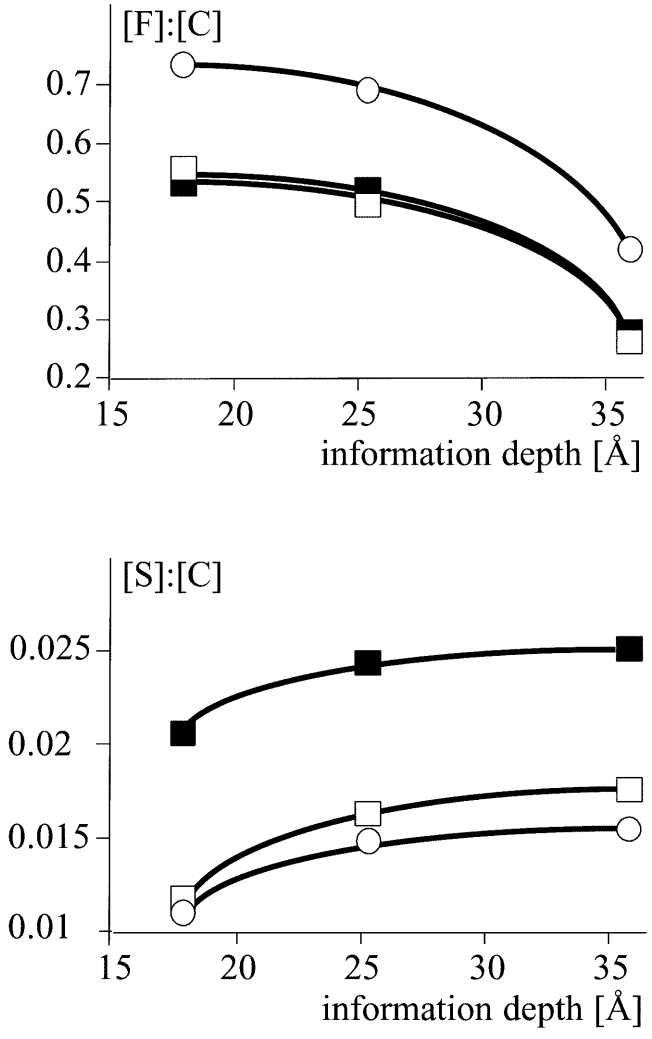

Fig. 3 F/C and S/C ratios as a function of sampling depth measured by angle-resolved XPS analysis for three block copolymers: BCP 1 (□); BCP 2 (■); BCP 3 (○)

Fig. 4 Tapping mode atomic force microscopy phase and height images for three block copolymers

Tapping mode AFM measurements

Tapping mode AFM was used to obtain height and phase images of the block copolymer surfaces. Typical results are shown in Fig. 4. The phase images (stiffness contrast) reveal that roughly spherical domains (dark) were formed on the surface of the thin block copolymer films. Since these domains are soft compared to the bright (hard) region they were assigned to components with relatively high amounts of fluorine. The semifluorinated polyester segments start softening above their glass transition temperature, which is around 0 °C. In contrast, the glass transition of the polysulfone matrix is at around 130 °C, i.e., the polysulfone component should be much harder than the semifluorinated polyester phase at ambient temperature. It was also found that the domains show lower adhesion than the matrix when phase imaging was used in adhesion contrast. This can be considered as an additional indication that the chemical composition of the domains is different from that of the matrix.

The spherical dark domains are well separated from each other and exhibit typical sizes (mean diameter) of 60–250 nm (Table 2). By changing the composition of the block copolymers the observed mean diameter of the soft domains is also changed (Fig. 4, Table 2). In addition, the surface ratio of the soft domains is increased by increasing the amount of the semifluorinated polyester segment in the bulk (Table 2). On several freshly prepared surfaces it could be shown that these results were reproducible.

Three-dimensional height images are shown in Fig. 4. For all three block copolymers, the S_a values were in the order of several nanometers on a 100 μm^2 image area (Table 2).

Discussion

Using XPS it could be shown in the present study that the advancing contact angle correlates directly with

Table 3 Bulk composition and surface properties of thin block copolymer films containing semifluorinated polyester segments

Block copolymer	Bulk composition			Water contact angle/solid surface tension		Elemental surface composition determined by X-ray photoelectron spectroscopy		
	M_n PSU	M_n SF-PES	Fluorine content (wt%)	θ_a (water)	γ_{sv} (EQS) (mJ/m^2)[a]	F/C	O/C	S/C
BCP 1	9000	830	4.1	111.6 ± 2.5	15.9 ± 1.4	0.56	0.15	0.02
BCP 2	2300	830	12.8	113.3 ± 1.2	14.9 ± 0.7	0.54	0.10	0.01
BCP 3	2300	3600	20.0	118.7 ± 0.6	12.0 ± 0.3	0.74	0.12	0.01

[a] Equation-of-state approach, Ref. [32]

Phase imaging, stiffness

Topography and roughness

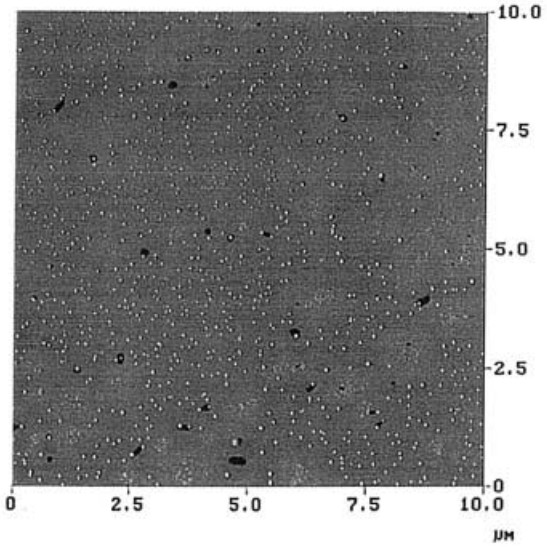

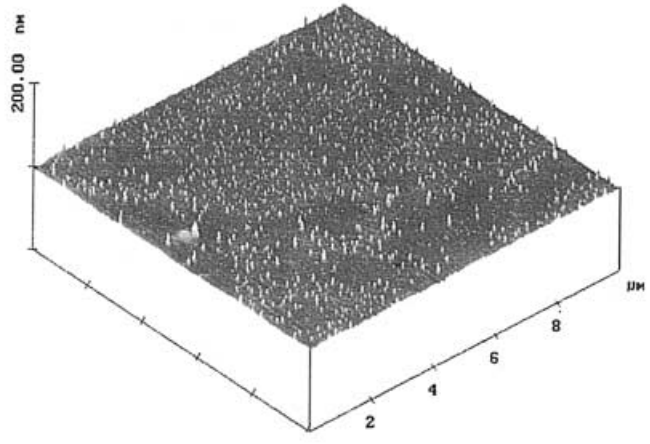

BCP 1 Roughness S_a= 0.9 nm

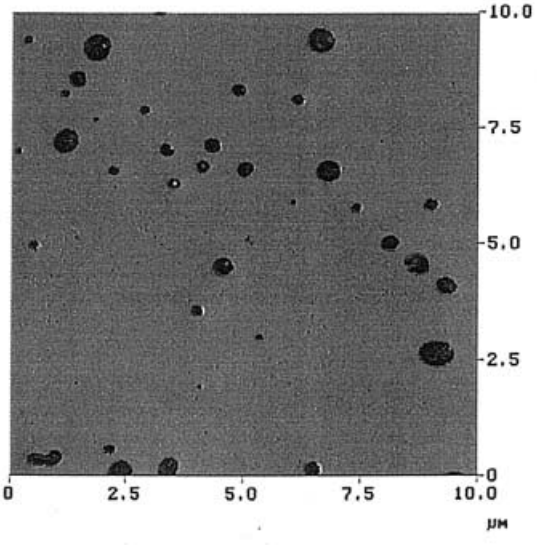

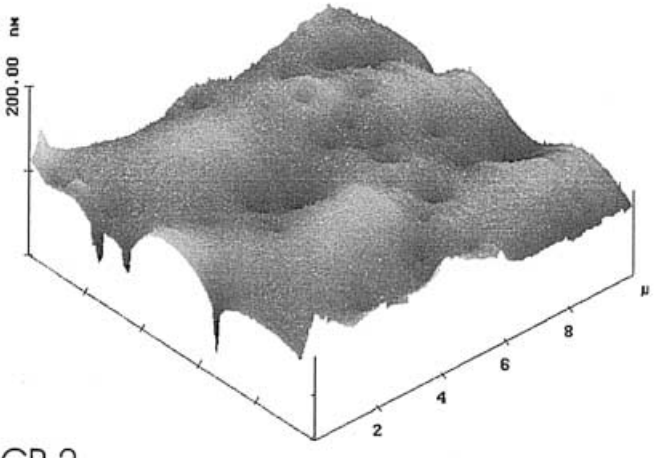

BCP 2 Roughness S_a= 11.3 nm

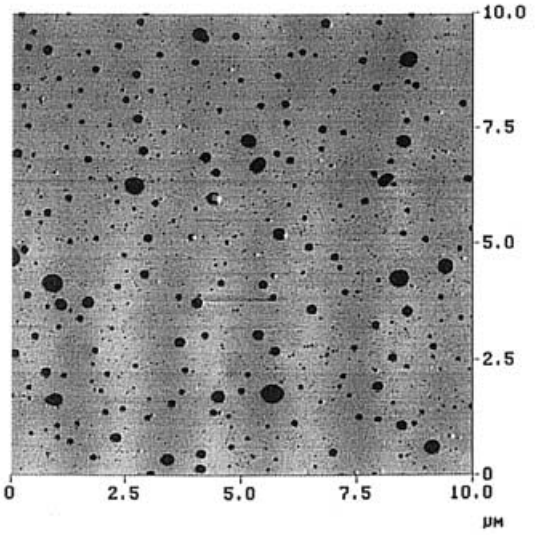

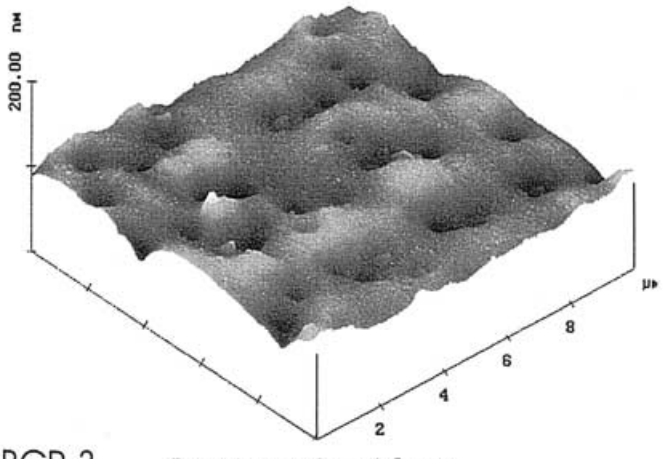

BCP 3 Roughness S_a= 4.9 nm

the fluorine content of the block copolymer surfaces (Table 3). Thus, if the fluorine content near the surface was essentially the same for two block copolymers (BCP 1 and BCP 2), then the advancing contact angles register this fact and yield nearly the same values. From the equality of the advancing contact angles on BCP 1 and BCP 2, another important conclusion can be drawn regarding the effect of the surface heterogeneity and roughness. Since both the BCP 1 and BCP 3 block copolymer surfaces differ in their roughness and heterogeneity, as established by AFM (Table 2, Fig. 4), the equality of the advancing contact angles indicates that neither roughness nor heterogeneity had a significant effect. It should be noted that these results were obtained for surfaces with roughness features on the nanometer length scale (S_a: 0.9–11.3 nm) and with heterogeneities on a submicrometer length scale (mean domain diameter about 60–250 nm).

At least, as far as heterogeneity is concerned, this result is not surprising. Since for BCP 1 and BCP 2 the global elemental surface composition is the same, differences could arise only if the three-phase line "recognized" the soft, hydrophobic domains, i.e., if the domains introduced contortions of the three-phase line. It has been argued repeatedly that such a recognition is intimately connected with line tension [20]. Such considerations about line tension can help to interpret our experimental results. A positive line tension will tend to counteract the tendency towards contortions of the three-phase line. Model calculations with heterogeneous solid surfaces [20] have shown that line tension will tend to minimize the length of the three-phase line in the same way as the surface tension tends to minimize the surface area of, say, a liquid drop. On the other hand, as a three-phase line crosses from one type of solid surface to another, say a more hydrophobic domain, the different equilibrium contact angles would, in the absence of line tension, mathematically cause a discontinuity in the curvature of the three-phase line. Physically, because of line tension, a balance is struck between the opposing forces such that the three-phase line reacts to a surface patch with a contorted shape. Since, for reasons of dimensionality, line tension appears in a product with the curvature of the line, this term can become so large for high curvatures, i.e., for small patches, that this highly curved system would be energetically unfavorable. Therefore, line tension will tend to cause the three-phase line to cut straight across small patches and, hence, to average over the two types of domains. From the point of view of contact angles, such surfaces are operationally homogeneous. With a line tension of 10^{-6} J/m [21], the lateral dimensions below which features, such as the soft domains, are not registered by the three-phase line have been estimated as 1 μm [20]. The domain diameters given in Table 1 are well below this value. Thus, our experimental results confirm the conclusion that heterogeneous polymer surfaces possessing patches, whose size is well below 1 μm in diameter, are operationally homogeneous from the point of view of macroscopic advancing contact angles.

Regarding the contact angle hysteresis, which was calculated as the difference between measured advancing and receding contact angles, we assume that liquid retention by the solid upon retraction of the three-phase line can help to explain the observed phenomena. It has become apparent recently [36] that a key cause for macroscopic contact angle hysteresis is liquid retention by the solid upon retraction of the three-phase line, even for very hydrophobic surfaces. Our results show that contact angle hysteresis increased with increasing percentage of the soft domains on the block copolymer surfaces (Table 2). If we are speculating on possible explanations for these observations then it would appear that on soft domains the liquid is retained in a different way than on the main surface phase. However, contact angle measurements on films of the pure semifluorinated polyester homopolymer and the pure high- molecular-weight polysulfone [35] do not reveal large differences in contact angle hysteresis. The contact angle hysteresis measured is in both cases about 30° using water as the liquid. However, it is also possible that, on the block copolymer surfaces, the borders between the two phases tend to retain liquid more strongly than a homogeneous surface would. This would explain the observed tendency of decreasing receding contact angles with increasing percentage of the soft domains. Since one would expect liquid retention to depend on such properties as the polarity and the molecular size of the liquid, further light will be shed on these difficult problems by using different liquids for the contact angle measurements. Using hexadecane as the measuring liquid, the observed contact angle hysteresis, $\Delta\theta$, was distinctly lower compared to water: for BCP 2 $\Delta\theta$ was found to be 10.2° and for BCP 3 the value was 13.2°. This small hysteresis for hexadecane makes good sense, since the relatively large size and the lack of polarity may not be conclusive to liquid retention.

Summary

The wettability on well-characterized heterogeneous surfaces of block copolymers has been studied using ADSA as a contact angle technique. The surface heterogeneity and roughness could be quantified by AFM. All the surfaces investigated had soft, hydrophobic domains of varying size on the submicrometer length scale and the mean roughness was of the order of several nanometers on a micrometer length scale. It was

found that neither roughness nor heterogeneity had a significant effect on the advancing contact angle of water, at the scale of the features present. These experimental results are in agreement with numerical calculations [20] which estimated the critical patch size on heterogeneous surfaces to be of the order of 1 μm, below which patches are not registered by the three-phase line.

Contact angle hysteresis increased with increasing percentage of the soft hydrophobic domains. A plausible explanation for this experimental finding can be liquid retention by the solid upon retraction of the three-phase line.

Concerning the molecular composition of these block copolymer surfaces, angle resolved XPS analysis showed a surface segregation of fluorine within the surface region. A direct correlation was found between the fluorine content of the block copolymer surfaces and the advancing contact angle of water.

Acknowledgements Financial support by the Deutsche Forschungsgemeinschaft (grant number Po 575/2-2) within the priority program Benetzung und Strukturbildung an Grenzflächen (SPP 1052) is gratefully acknowledged. The silicon wafers used as substrates to prepare the polymer films were kindly supplied by Wacker Siltronic, Germany.

Appendix
Synthesis of block copolymers

A typical polycondensation procedure is described in the following. Acetylated polysulfone with a molecular weight of 2370 g/mol (0.694 g; 0.000302 mol) and semifluorinated isophthalic acid (0.253 g; 0.000302 mol) are placed into a three-necked flask with a nitrogen inlet, a stirrer and a distillation head. After purging the flask with nitrogen for 1 h., the flask is immersed in a metal bath preheated to 200 °C. The reaction is started by stirring and under nitrogen flow. After 5 min, the temperature is raised to 260 °C for a further 25 min. After that time, a vacuum (133 Pa) is applied. The polycondensation is finished after a further 3 h and the flask is removed from the metal bath and the polymer is removed from the flask mechanically.

References

1. Kobyashi H, Owen MJ (1995) Trends Polym Sci 3:330
2. Schmidt DL, Coburn CE, Dekoven BM, Potter GE, Meyers GF, Fisher DA (1994) Nature 368:39
3. Chapman TM, Marra KG (1995) Macromolecules 28:2081
4. Lenk TL, Hallmark VM, Hoffmann CL, Rabolt JF, Castner DG, Erdelen C, Ringsdorf H (1994) Langmuir 10:4610
5. Hwang SS, Ober CK, Perutz S, Iyengar D, Schneggenburger LA, Kramer EJ (1995) Polymer 36:1321
6. Wang J, Ober CK (1997) Macromolecules 30:7560
7. Höpken J, Möller M (1992) Macromolecules 25:1461
8. Lindner E (1992) Biofouling 6:193
9. Krupers MJ, Möller M (1997) J Fluorine Chem 82:119
10. Sheiko S, Lermann E, Möller M (1996) Langmuir 12:4015
11. Wang J, Mao G, Ober CK, Kramer EJ (1997) Macromolecules 30:1906
12. Pospiech D, Jehnichen D, Häussler L, Voigt D, Grundke K, Ober CK, Körner H, Wang J (1998) Polym Prepr Am Chem Soc Div Polym Chem 3:882
13. Johnson RE Jr, R. Dettre H (1964) J Phys Chem 68:1744
14. Yang XF (1995) Appl Phys Lett 67:2249
15. de Gennes PG (1985) Rev Mod Phys 57:827
16. Eick JD, Good RJ, Neumann AW (1975) J Colloid Interface Sci 53:235
17. Schwartz LW, Garoff S (1985) Langmuir 1:219
18. Hellwig GEH, Neumann AW (1969) Kolloid Z Z Polym 40:229
19. Herzberg WJ, Marian JE, Vermeulen (1970) J Colloid Interface Sci 33:1
20. Gaydos J, Neumann AW (1996) In: Neumann AW, Spelt JK (eds) Applied surface thermodynamics. Dekker, New York, pp 169–238
21. Amirfazli A, Kwok DY, Gaydos J, Neumann AW (1998) J Colloid Interface Sci 205:1
22. Fadeev AY, McCarthy TJ (1999) Langmuir 15:3759
23. Öner D, McCarthy TJ (2000) Langmuir 16:7777
24. Sheiko SS, Möller M, Cantow H-J, Magonov SN (1993) Polym Bull 31:693
25. van den Berg R, de Groot H, van Dijk MA, Denley DR (1994) Polymer 35:5778
26. Krausch G, Hipp M, Böltau M, Marti O, Mlynek J (1995) Macromolecules 28:6773
27. Magonov SN, Elings V, Papkov VS (1997) Polymer 38:297
28. Lahooti S, del Rio OI, Cheng P, Neumann AW (1996) In: Neumann AW, Spelt JK (eds) Applied surface thermodynamics. Dekker, New York, pp 441–507
29. Cheng P, Li D, Boruvka L, Rotenberg Y, Neumann AW (1990) Colloids Surf 43:151
30. Kwok DY, Gietzelt T, Grundke K, Jacobasch HJ, Neumann A (1997) Langmuir 13:2880
31. Augsburg A, Grundke K, Pöschel K, Jacobasch HJ, A. Neumann AW (1998) Acta Polym 49:417
32. Kwok DY, Neumann AW (1999) Adv Colloid Interface Sci 81:167
33. Pospiech D, Eckstein K, Komber H, Voigt D, Böhme F, Kricheldorf HR (1997) Polym Prepr Am Chem Soc Div Polym Chem 38:398
34. Seah MP (1990) In: Briggs D, Seah MP (eds) Practical surface analysis by Auger and X-ray photoelectron spectroscopy. Wiley, Chinchester, pp 202–255
35. Pospiech D, Eckstein K, Häussler L, Komber H, Jehnichen D, Grundke K, Simon F (1999) Macromol Chem Phys 200:1311
36. Sedev RV, Petrov JG, Neumann AW (1996) J Colloid Interface Sci 180:36